AD

CONTRACT REPORT ARBRL-CR-00521

ARC-DYNAMIC CALCULATIONS IN THE RAIL GUN

Prepared by

Science Applications, Inc.
1503 Johnson Ferry RD, Suite 100
Marietta, GA 30062

November 1983

US ARMY ARMAMENT RESEARCH AND DEVELOPMENT CENTER
BALLISTIC RESEARCH LABORATORY
ABERDEEN PROVING GROUND, MARYLAND

Destroy this report when it is no longer needed.
Do not return it to the originator.

Additional copies of this report may be obtained from the National Technical Information Service, U. S. Department of Commerce, Springfield, Virginia 22161.

The findings in this report are not to be construed as an official Department of the Army position, unless so designated by other authorized documents.

The use of trade names or manufacturers' names in this report does not constitute indorsement of any commercial product.

UNCLASSIFIED

SECURITY CLASSIFICATION OF THIS PAGE *(When Data Entered)*

REPORT DOCUMENTATION PAGE		READ INSTRUCTIONS BEFORE COMPLETING FORM
1. REPORT NUMBER CONTRACT REPORT ARBRL-CR-00521	2. GOVT ACCESSION NO.	3. RECIPIENT'S CATALOG NUMBER
4. TITLE *(and Subtitle)* ARC-DYNAMIC CALCULATIONS IN THE RAIL GUN		5. TYPE OF REPORT & PERIOD COVERED Final
		6. PERFORMING ORG. REPORT NUMBER
7. AUTHOR(s) Jad H. Batteh		8. CONTRACT OR GRANT NUMBER(s) DAAK11-82-C-0086
9. PERFORMING ORGANIZATION NAME AND ADDRESS Science Applications, Inc. 1503 Johnson Ferry RD, Suite 100 Marietta, GA 30062		10. PROGRAM ELEMENT, PROJECT, TASK AREA & WORK UNIT NUMBERS
11. CONTROLLING OFFICE NAME AND ADDRESS US Army AMCCOM, ARDC Ballistic Research Laboratory, ATTN: DRSMC-BLA-S(A) Aberdeen Proving Ground, MD 21005		12. REPORT DATE November 1983 13. NUMBER OF PAGES 53
14. MONITORING AGENCY NAME & ADDRESS*(if different from Controlling Office)*		15. SECURITY CLASS. *(of this report)* UNCLASSIFIED 15a. DECLASSIFICATION/DOWNGRADING SCHEDULE

16. DISTRIBUTION STATEMENT *(of this Report)*

Approved for public release; distribution unlimited.

17. DISTRIBUTION STATEMENT *(of the abstract entered in Block 20, if different from Report)*

18. SUPPLEMENTARY NOTES

19. KEY WORDS *(Continue on reverse side if necessary and identify by block number)*

Electric gun	Fluid mechanics
Rail gun	Lorentz force
Electromagnetic propulsion	Rail damage
Plasma dynamics	Rail erosion

20. ABSTRACT *(Continue on reverse side if necessary and identify by block number)*

In several models of arc-driven rail guns, the rails are assumed to be infinitely high to simplify the calculation of the electromagnetic fields in the arc. This assumption overestimates the arc pressures and accelerations by approximately a factor of two for typical rail gun geometries. In this report, we develop a simple method for modifying the infinite-height models to account for the effect of finite-height rails on the performance of the rail gun and the properties of the arc. The modification is based on an integration of the

DD FORM 1 JAN 73 1473 EDITION OF 1 NOV 65 IS OBSOLETE

UNCLASSIFIED

SECURITY CLASSIFICATION OF THIS PAGE *(When Data Entered)*

Lorentz force across the arc cross section at each axial location in the arc. Application of this technique suggests that, for typical rail gun geometries, the variation of the arc pressure (averaged over the arc cross section) can be well approximated by merely scaling the pressure profile for the case of infinite-height rails, the scaling factor being a function of the effective inductance for the finite-height geometry. Exploiting this result in a simple arc model for the Rashleigh-Marshall experiment, we find that use of the finite-height model leads to considerably lower predictions for the arc pressure, density, acceleration, and arc mass when compared to the predictions of the infinite-height model for the same arc length. On the other hand, the use of a finite-height rail gun model leads to a higher prediction for the arc muzzle voltage. A review of models which have recently been proposed for analyzing mechanical and thermal damage to the rails in arc-driven rail guns is also presented, and recommendations for future theoretical and experimental investigations of arc-driven rail guns are proposed.

TABLE OF CONTENTS

THIS PAGE WAS INTENTIONALLY LEFT BLANK

LIST OF FIGURES

THIS PAGE WAS INTENTIONALLY LEFT BLANK

LIST OF TABLES

THIS PAGE WAS INTENTIONALLY LEFT BLANK

I. INTRODUCTION

Research conducted over the past decade has demonstrated that electromagnetic propulsion is a viable technology for accelerating macroscopic projectiles to very high velocities. Particularly noteworthy are the achievements in rail gun technology, whose modern history began with the work of Marshall and his co-workers [1-3] at the Australian National University. The state-of-the-art in rail gun technology is exemplified by the recently completed program, sponsored jointly by DARPA and the U.S. Army Armament Research and Development Command, in which a five-meter rail gun built by Westinghouse was used to accelerate a 317-g projectile to 4.2 km/s [4].

Although this particular experiment utilized a solid armature, it is generally recognized that the push to ever higher velocities will require the use of plasma armatures, both to circumvent the problem of solid armature breakup and melting at high driving currents and to help insure good contact between the armature and rails at high projectile velocities. Consequently, considerable effort has been expended in the theoretical and experimental study of arc-driven rail guns.

Included among the theoretical studies of arc armatures are the analyses of Powell and Batteh [5-7], which are based primarily on two assumptions - (1) that the arc is steady in a reference frame that accelerates with the arc/projectile system, and (2) that the rail height is much greater than the rail separation. The first assumption is probably reasonable once the effects of the initiation sequence used to generate the arc have dissipated. The second, however, is decidedly not valid since rail gun geometries typically have comparable values for the rail spacing and rail height.

---

1. J.P. Barber, 'The Acceleration of Macroparticles and a Hypervelocity Electromagnetic Accelerator,' Ph.D. Thesis (Australian National University, 1972) (Unpublished).

2. R.A. Marshall, 'The Australian National University Rail Gun Project,' Atomic Energy 16, January 1975.

3. S.C. Rashleigh and R.A. Marshall, 'Electromagnetic Acceleration of Macroparticles to High Velocities,' J. Appl. Phys. 49, 2540 (1978).

4. 'Laboratory Demonstration Electromagnetic Launcher - EMACK,' Commissioning Test Results, Westinghouse Research and Development Center, Pittsburgh, PA.

5. J.D. Powell and J.H. Batteh, 'Plasma Dynamics of an Arc-Driven, Electromagnetic Projectile Accelerator,' J. Appl. Phys. 52, 2717 (1981).

6. J.H. Batteh, 'Analysis of a Rail Gun Plasma Accelerator,' Science Applications, Inc., Ballistic Research Laboratory Contract Report No. ARBRL-CR-00478, 1982 (AD A114043).

7. J.D. Powell and J.H. Batteh, 'Two-Dimensional Plasma Model for the Arc-Driven Rail Gun,' J. Appl. Phys. 54, 2242 (1983).

The two major objectives of the effort conducted under this contract were (1) to develop a simple method for modifying the analyses in Refs. 5-7 to account for finite-height rails, and (2) to determine the extent to which including this effect alters the predictions of arc properties. A third objective was to review the studies of heat transfer and erosion in conventional gun tubes and assess their applicability to the study of damage to the rails in rail guns. Another task undertaken during this contract period was a joint study with John Powell of the Ballistic Research Laboratory of the limitations imposed on projectile acceleration by the atmosphere in a non-evacuated rail gun. Since the results of this latter task will be published elsewhere [8], only the results of the first three tasks will be presented in this report.

The report is organized as follows: In Section II we investigate the effect of finite-height rails on the net accelerating force in the rail gun, based on the integration of the Lorentz force over the cross section of the armature. From this analysis we derive an expression for the effective inductance per unit length of the gun, which is a function of the geometry of the rails and armature. Our equation for the inductance is actually more general than Niwa's often used formula, found in the text by Grover [9], since we allow the height of the armature on the rails to be different from the rail height. In Section III we develop a simple method for incorporating the effects of finite-height rails into the analysis of rail gun arcs. In addition, we show that for typical rail gun geometries, the momentum equation which describes the pressure variation in the arc can be well approximated by merely scaling the corresponding equation obtained for the case of infinitely high rails. We exploit this result in Section IV where we use a modification of the analysis of Ref. 6 to determine the effect of finite-height rails on arc properties. Section V contains a brief discussion of the mechanisms responsible for gun tube erosion, and contrasts these with the mechanisms most likely to result in damage to the rails in arc-driven rail guns. This section also contains a discussion of some recent models developed to analyze mechanical and thermal damage in rail guns. Section VI contains a summary and discussion of the work presented in this report, as well as recommendations for future studies.

8. J.D. Powell and J.H. Batteh, 'Atmospheric Effects on Projectile Acceleration in the Rail Gun,' J. Appl. Phys (in press).

9. F.W. Grover, Inductance Calculations (Van Nostrand, New York, 1946) Ch. 10.

II. EFFECTIVE INDUCTANCE CALCULATION

In this section, we present a derivation for the effective inductance per unit length (hereafter referred to as the inductance) of a rail gun with finite-height rails. This inductance, denoted by L, is defined such that the net accelerating Lorentz force on the armature and projectile is given, for a fixed geometry and constant current, by

$$F = LI_o^2/2 \tag{2-1}$$

where I_o is the magnitude of the current in the rails.

The geometry used in the calculation is shown in Fig. 1. In the figure, x_o denotes the distance from the power supply to the armature, w is the rail separation, and h_a is the height of the armature on the rails, which in general will be different from the rail height, h_r.

For typical rail gun configurations, the length of the gun far exceeds the rail height and separation. Thus, for most of the acceleration process $x_o \gg h_r$ and w and the rails can be assumed to extend to $-\infty$ in the x-direction. We incorporate this assumption into the analysis and assume, in addition, that the current is carried on the inner surface of the rails. The x-component of the current in the rails is taken to be uniformly distributed on the rails.

The armature is assumed to carry a current only in the y-direction, the current being distributed uniformly along the inner surface of the armature. Thus, we can write the armature current density as

$$\vec{J}_a(x,y,z) = J_{ay}(y,z)\,\delta(x-x_o)\vec{y} \tag{2-2}$$

where δ is the delta function and

$$J_{ay} = \begin{cases} -I_o/h_a, & |y| \le w/2,\ |z| \le h_a/2 \\ 0, & \text{otherwise} \end{cases}.$$

Calculating the inductance based on a current which flows only on the surface of the armature is not as restrictive as one might guess. In Ref. 10 it was shown that for $h_a = h_r = \infty$ the net accelerating

10. J.D. Powell and J.H. Batteh, 'Plasma Dynamics of the Arc-Driven Rail Gun,' Ballistic Research Laboratory Report No. ARBRL-TR-02267, 1980 (AD A092345).

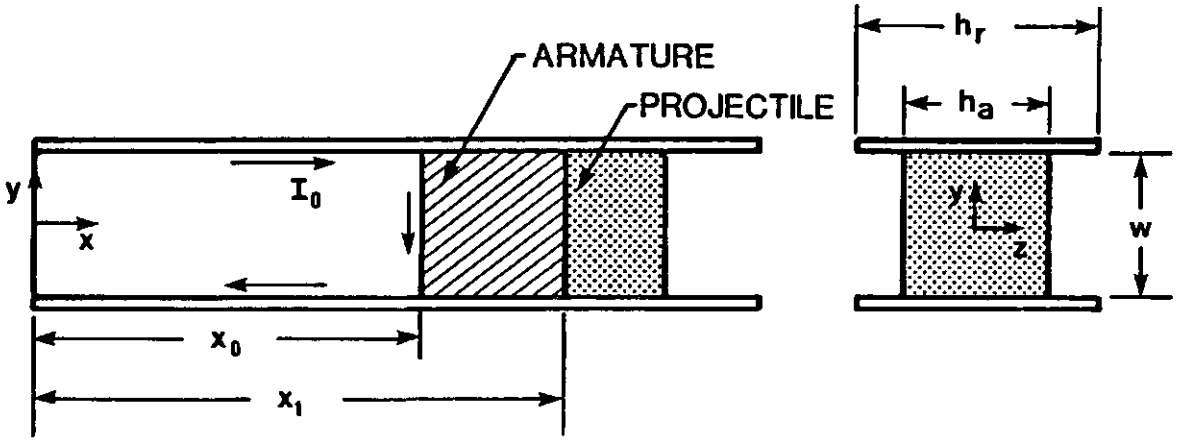

Figure 1. Rail Gun Model for Inductance Calculation

pressure on the armature, and thus the effective inductance, are independent of the distribution of the armature current in the axial direction (x-direction). A similar result, based on the analysis of Section III of this report, is derived in the Appendix for the case where h_a and h_r are equal but finite. We have not attempted to prove this result for the more general case where $h_a \neq h_r$, but these analyses suggest its validity.

The current density in the rails is

$$\vec{J}_r(x,y,z) = \left[\delta(y-w/2) - \delta(y+w/2)\right]\left[J_{rx}(x,z)\vec{x} + J_{rz}(x,z)\vec{z}\right] \quad . \quad (2\text{-}3)$$

Because of our assumption that the x-component of the current is uniformly distributed on the rails,

$$J_{rx}(x,z) = \begin{cases} I_o/h_r & , \; x < x_o, \; |z| \leq h_r/2 \\ 0 & , \; \text{otherwise} \quad . \end{cases} \quad (2\text{-}4)$$

J_{rz} is obtained from the current continuity equation,

$$\vec{\nabla} \cdot \vec{J} = 0 \quad . \quad (2\text{-}5)$$

In writing Eq. (2-5), we have neglected the contribution of the displacement current, which is valid for nonrelativistic projectile velocities. Substituting the equations for J_a and J_r into Eq. (2-5) yields an ordinary differential equation for J_{rz}. Solving this equation subject to the conditions that J_{rz} be continuous at $z = h_a/2$ and vanish at $z = 0$ yields

$$J_{rz}(x,z) = -I_o/h_a \; \delta(x-x_o) \begin{cases} 0 & , \; |z| > h_r/2 \\ -h_a/h_r \; (z + h_r/2), & -h_r/2 \leq z \leq -h_a/2 \\ (1 - h_a/h_r)z & , \; |z| < h_a \\ h_a/h_r \; (h_r/2 - z) & , \; h_a/2 \leq z \leq h_r/2 \quad . \end{cases} \quad (2\text{-}6)$$

Actually, J_{rz} is presented here only for completeness since it will not contribute to the accelerating force because of our assumption that the current in the armature has only a y-component. Thus, only the component of the magnetic induction in the z-direction, B_z, can contribute to a force in the armature in the x-direction.

To calculate the effective inductance, we first calculate the net force in the z-direction on the armature from the Lorentz law, which for our model reduces to

$$F_x = -\frac{I_o}{h_a}\int_{-w/2}^{w/2}\int_{-h_a/2}^{h_a/2} B_z(x_o,y,z)\,dz\,dy \quad , \tag{2-7}$$

and then use Eq. (2-1) to obtain L. In this report, we shall use the notation $\langle A(x)\rangle$ to denote the average of A over the plane of the armature located at x, i.e.,

$$\langle A(x)\rangle = \frac{1}{wh_a}\int_{-w/2}^{w/2}\int_{-h_a/2}^{h_a/2} A(x,y,z)\,dz\,dy \quad . \tag{2-8}$$

Using this notation, we can write F_x as

$$F_x = -wI_o\,\langle B_z(x_o)\rangle \tag{2-9}$$

and the effective inductance as

$$L = 2w\,\langle B_z(x_o)\rangle / I_o . \tag{2-10}$$

Since the armature current cannot exert a net force upon itself, only the rail currents need to be considered in deriving $\langle B_z(x_o)\rangle$. Calculating B_z due to the rail currents for a point on the surface of the armature from the Biot-Savart law yields

$$B_z(x_o,y,z) = \frac{\mu I_o}{4\pi h_r}\int_{-\infty}^{x_o}\int_{-h_r/2}^{h_r/2}\left[\frac{y-w/2}{r_1^2} - \frac{y+w/2}{r_2^2}\right]dz'dx' \tag{2-11}$$

where $\mu = 4\pi \times 10^{-7}$ H/m is the permeability of free space, and r_1 and r_2 are given by

$$r_1 = \left[(x_o - x')^2 + (y - w/2)^2 + (z - z')^2\right]^{1/2}$$

$$r_2 = \left[(x_o - x')^2 + (y + w/2)^2 + (z - z')^2\right]^{1/2}. \qquad (2\text{-}12)$$

Carrying out the integration yields

$$B_z(x_o,y,z) = \frac{\mu I_o}{4\pi h_r}\left[\tan^{-1}\left(\frac{2z-h_r}{2y-w}\right) - \tan^{-1}\left(\frac{2z+h_r}{2y-w}\right) + \tan^{-1}\left(\frac{2z+h_r}{2y+w}\right) - \tan^{-1}\left(\frac{2z-h_r}{2y+w}\right)\right]. \qquad (2\text{-}13)$$

Averaging Eq. (2-13) over the armature cross section and substituting into Eq. (2-10) yields the following expression for the effective inductance

$$L = \frac{2\mu w^2}{\pi h_r h_a}\left[I\left(\frac{h_r+h_a}{2w}\right) - I\left(\frac{h_r-h_a}{2w}\right)\right] \qquad (2\text{-}14)$$

where

$$I(s) = s\tan^{-1}(s) + s^2/4\ \ln(1 + 1/s^2) - 1/4\ \ln(1 + s^2). \qquad (2\text{-}15)$$

As mentioned previously, Niwa has calculated an expression for the effective inductance of a rectangular current sheet, which is presented in the text by Grover [9]. Our result, Eq. (2-14), agrees numerically with Niwa's formula when h_r is equal to h_a and when Niwa's formula is applied in the limit of infinitely long rails.

It is apparent from Eqs. (2-14) and (2-15) that the inductance is a function only of the rail height ratio, h_r/w, and the arc height ratio, h_a/h_r. This functional dependence is depicted in Fig. 2 where we have plotted the inductance as a function of the rail height ratio for $h_a/h_r = 0.5$ and 1.0. Also marked in the figure are the theoretical predictions for the geometry of the Rashleigh-Marshall (RM) experiment [3] ($h_r/w = 1.5$, $h_a/h_r = 0.67$) and the Ballistic Research Laboratory (BRL) experiments [11] ($h_r/w = 2.0$, $h_a/h_r = 0.5$).

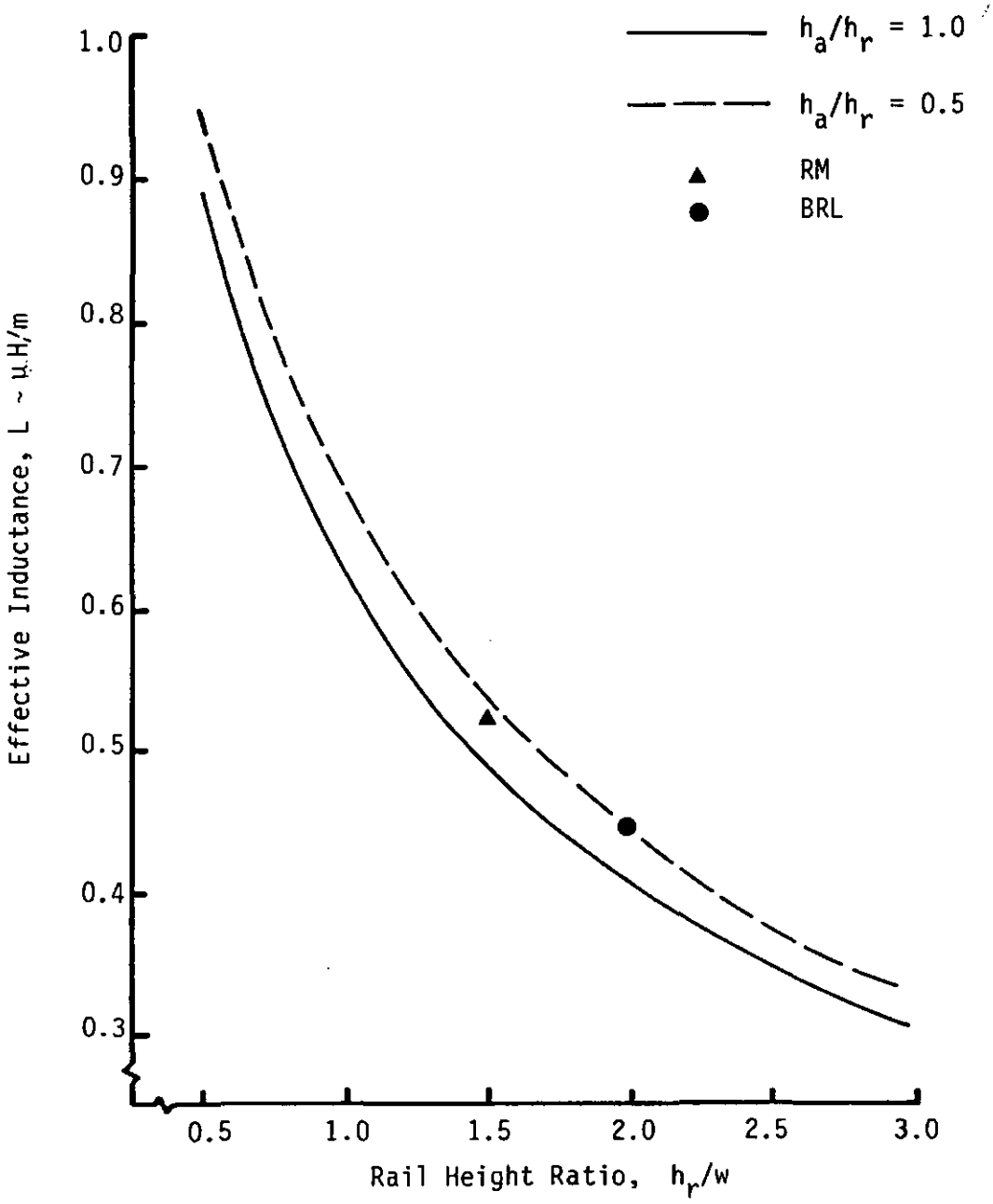

Figure 2. Effective Inductance for Finite-Height Rail Guns

Figure 2 indicates that considerable error can be introduced if Niwa's formula, which corresponds to the solid curve in the figure, is not used judiciously. For example, if we apply Niwa's formula to the BRL tests by assuming that h_a and h_r are equal to the arc height, then we obtain a value of L equal to 0.628 μH/m, which is considerably greater than the value of 0.444 μH/m predicted for $h_a/h_r = 0.5$. Somewhat better agreement is obtained if both heights are assumed equal to the rail height. But in this case, one must be careful to apply the force to the actual armature cross-sectional area in order to obtain accurate predictions for the pressure on the armature.

In previous studies, Powell and Batteh have attempted to simulate the RM experiment based on a rail gun model which assumes, for computational simplicity, that the rails are infinitely high [5]. As discussed in Ref. 6, this assumption, for a current per unit height equal to that of the RM experiment, overestimates the arc pressure and acceleration by approximately a factor of two. In fact, to obtain the same pressure as that predicted from the infinite-height model from Eq. (2-1) and the actual RM geometry would require an effective inductance on the order of 1μH/m. Equation 2-14, on the other hand, predicts a considerably lower value, 0.526 μH/m, for the RM geometry. Thus, we expect that the pressures and accelerations predicted in the earlier studies are inaccurate. This point will be addressed in greater detail in the following section. It is perhaps worth mentioning that in Ref. 6, an effective inductance of 0.53 μH/m was estimated for the RM experiment based on the experimentally measured current profile and projectile acceleration. This value is essentially identical to the theoretical calculation based on Eq. (2-14). We suspect, however, that the remarkable agreement may be fortuitous to some extent since the model leading to Eq. (2-14) does not account for frictional drag on the projectile and for the modification of the inductance due to the diffusion of current in the rails, both of which are implicitly included in the calculation based on the experimentally measured parameters.

The theory developed in this section also provides a measure of the nonuniformity of the accelerating force, which is often an important factor in projectile/armature design. Because of our assumption that the current is uniform on the surface of the armature, the ratio of the pressure at any point on the armature surface to the average pressure is proportional to the ratio of the magnetic induction at that point to the average induction, i.e.,

$$p(x_o,y,z)/\langle p(x_o)\rangle = B_z(x_o,y,z)/\langle B_z(x_o)\rangle. \qquad (2\text{-}16)$$

It can be readily shown by differentiation of Eq. (2-13) that the peak pressure occurs at $x = 0$, $y = \pm w/2$. Consequently, the peak to average pressure on the projectile can be written as:

$$\frac{p_{max}}{p_{avg}} = \frac{\mu w}{2\pi h_r L} \left[\pi + 2 \tan^{-1} \frac{h_r}{2w} \right] . \qquad (2\text{-}17)$$

Again, it is clear that the pressure ratio depends only on the rail height ratio and the arc height ratio.

Figure 3 shows plots of the pressure ratio, as determined from Eq. (2-17), which correspond to the inductance plots of Fig. 2. Figures 2 and 3 clearly demonstrate the well-known fact that the effective inductance, and thus the accelerating force for a given current, increase with decreasing rail height ratio, but that this increase is obtained at the expense of a greater nonuniformity in the pressure on the armature. On the other hand, the figures indicate that for a given rail height ratio, the effective inductance actually increases somewhat as h_a/h_r is reduced, while a substantial improvement in pressure uniformity is achieved. While this suggests that there may be an advantage to designs employing a low h_a/h_r, it should be noted that decreasing h_a/h_r for a given h_r will also cause an increase in p_{avg} since a larger force will be applied to a smaller cross-sectional area. In addition, there will be increased ohmic losses per unit volume in the armature and rail as the current constricts to adjust to the armature height.

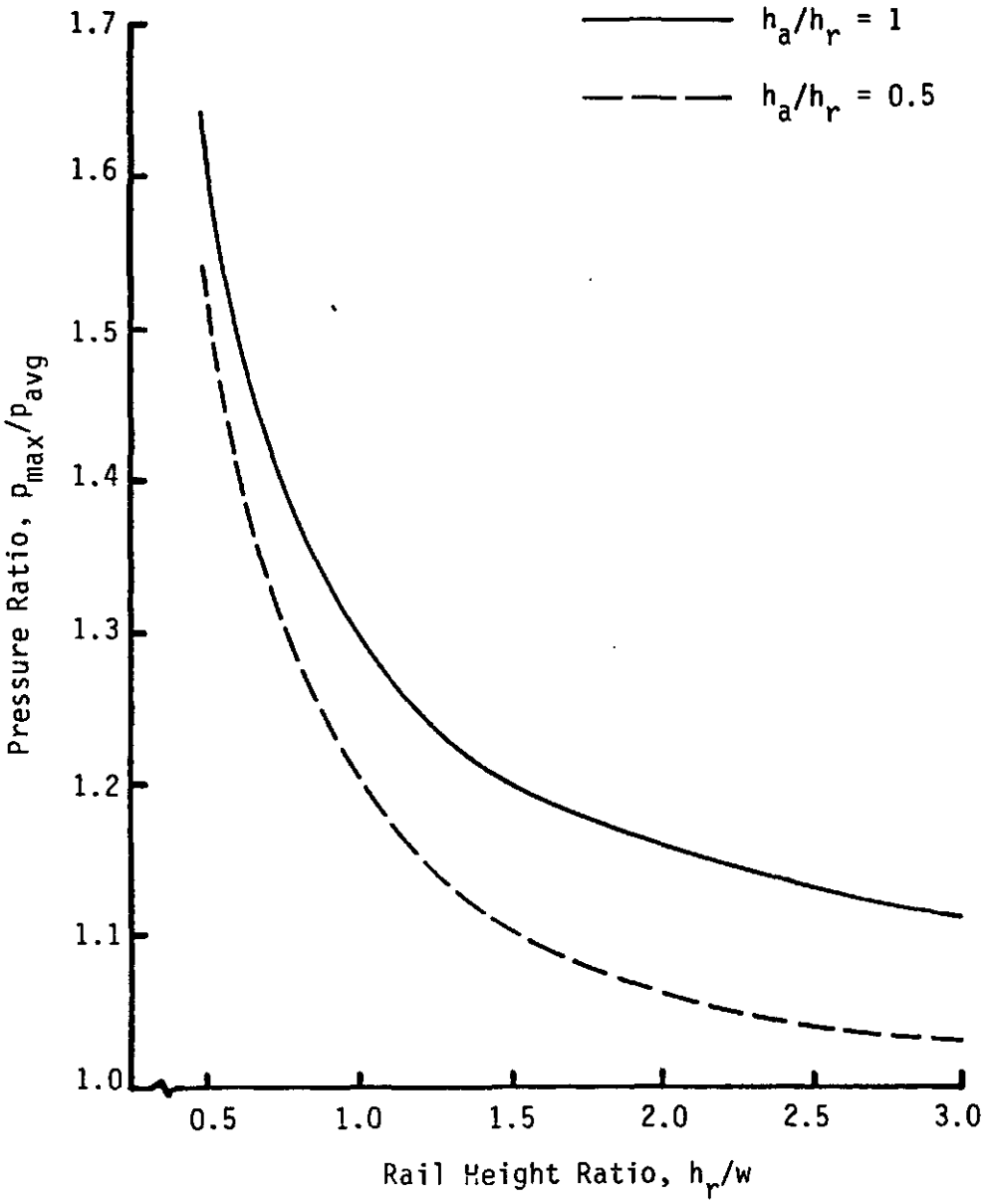

Figure 3. Pressure Ratio for Finite-Height Rail Guns

III. MODELING THE ARC DYNAMICS OF FINITE-HEIGHT ARC-DRIVEN RAIL GUNS

Previous analyses of arc-driven rail guns have invoked the assumption that the rail height, h_r, and arc height, h_a, are infinite [5-7]. This assumption leads to a considerable simplification in the momentum equation describing the arc.

Consider, for example, the model shown in Fig. 1 where we take the armature to be an arc with length $\ell_a = x_1 - x_o$. We assume that the arc is steady in a frame accelerating with the arc/projectile system and that the thermodynamic properties of the arc are functions only of x. Then, if the arc and rail heights are infinite, the magnetic induction field is independent of y and z and the axial momentum equation in the accelerating frame becomes [5]

$$dp/d\xi = \ell_a [J_y(\xi)B_z(\xi) - \rho(\xi)a] \tag{3-1}$$

where p is the pressure in the arc, J_y is the current density in the arc in the y-direction, ρ is the density, a is the common arc/projectile acceleration and

$$\xi = (x - x_o)/\ell_a \tag{3-2}$$

is the non-dimensional distance measured from the back of the arc. Furthermore, the current density and magnetic induction are defined by

$$J_y(\xi) = -\frac{\sigma(\xi) j_o}{\ell_a \bar{\sigma}} \tag{3-3}$$

$$B_z(\xi) = \mu \ell_a \int_\xi^1 J_y(\xi)\, d\xi \tag{3-4}$$

where σ is the conductivity of the arc, $\bar{\sigma}$ is the average conductivity of the arc

$$\bar{\sigma} = \int_o^1 \sigma(\xi)\, d\xi \tag{3-5}$$

and

$$j_o = I_o/h_a \tag{3-6}$$

is the current per unit height of the rail.

As formulated in Eq. (3-1), the pressure for the infinite-height rail gun is assumed to be a function only of the axial coordinate. This assumption is not valid for rail guns with finite-height since both J_y and B_z depend on z and y, as well as x. On the other hand, Eq. (3-1) will be a valid representation for the <u>average</u> pressure on a cross section of the arc in a finite-height gun, provided that the term $J_y B_z$ in that equation is replaced by the average of the product over the cross section.* Unfortunately, the exact calculation of this average would entail a detailed solution of Maxwell's equations in three dimensions.

To avoid this complication, we proceed in the following manner. First, we assume that the current in the arc flows only in the y-direction and is uniform across the arc cross section. We take its value to be the average value of J_y over that cross section. We then estimate the average pressure on the arc cross section according to the equation

$$d\langle p\rangle/d\xi = \ell_a \left[\langle J_y\rangle \langle B_z\rangle - \rho(\xi) a \right] \qquad (3\text{-}7)$$

where $\langle B_z\rangle$ is calculated based on the current distribution $\langle J_y\rangle$.

The average arc current is given by

$$\langle J_y\rangle = \sigma(\xi) \left(\langle E_y\rangle - v\langle B_z\rangle\right) , \qquad (3\text{-}8)$$

where v is the material velocity of the arc and projectile in the x-direction, and $\langle E_y\rangle$ is the average electric field in the y-direction. $\langle E_y\rangle$ is derived from Maxwell's equation

$$\vec{\nabla} \times \vec{E} = - \partial\vec{B}/\partial t \ . \qquad (3\text{-}9)$$

Recalling that our system is steady in the accelerating frame and transforming to that frame, we find that the z-component of Eq. (3-9) reduces to

$$\partial E_y/\partial\xi - \ell_a \, \partial E_x/\partial y = v \, \partial B_z/\partial\xi \ . \qquad (3\text{-}10)$$

It should be noted that, although we have transformed to the accelerating frame, the electromagnetic fields in Eq. (3-10) are those measured by an observer in the fixed frame.

---

*Actually, an additional term should be included in Eq. (3-1) consisting of the product of J_z and B_y, but this term should be much less than the $J_y B_z$ product for typical rail gun geometries.

Averaging Eq. (3-10) over the arc surface at each ξ-plane and noting that E_x vanishes at the surface of the perfectly conducting rails, yields

$$d\langle E_y\rangle/d\xi = v\, d\langle B_z\rangle/d\xi \quad . \tag{3-11}$$

The solution to Eq. (3-11) is

$$\langle E_y\rangle = v\langle B_z\rangle + E_o \tag{3-12}$$

where E_o is a constant. Substituting Eq. (3-12) into Eq. (3-8) and using the current conservation relation

$$\int_o^1 \langle J_y\rangle\, d\xi = -\frac{j_o\, h_r}{\ell_a\, h_a} \tag{3-13}$$

yields

$$E_o = -\frac{j_o\, h_r}{\ell_a\, h_a\, \bar{\sigma}} \tag{3-14}$$

and

$$\langle J_y\rangle = -\frac{j_o\, h_r}{\ell_a\, h_a\, \bar{\sigma}}\, \sigma(\xi) \quad . \tag{3-15}$$

Except for the factor h_r/h_a, Eq. (3-15) is identical to the result obtained for the arc current density in an infinite-height rail gun [5].

We now proceed to the calculation of $\langle B_z\rangle$ for the current profile $\langle J_y\rangle$. For simplicity, we limit our discussion to the case where $h_r = h_a$ and denote this common value by h. Figure 4 shows a circuit which encompasses a portion of the arc. The circuit is parallel to the rails, has a height corresponding to the arc height h_a, and extends to infinity in the x-direction. Applying Ampere's law to this circuit and noting that the electromagnetic fields must vanish at infinity yields

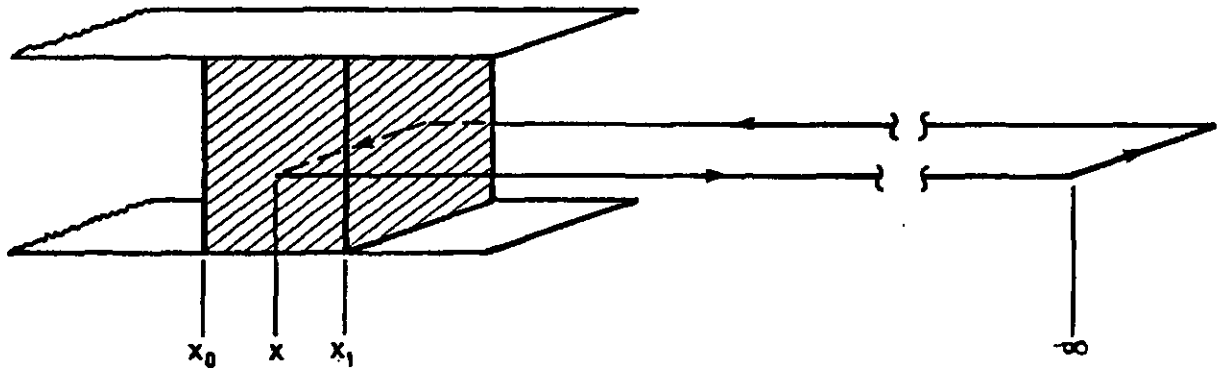

Figure 4. Circuit Geometry for Magnetic Induction Calculation

$$\int_{-h/2}^{h/2} B_z(x,y,z)\, dz \;=\; \mu h \int_{x}^{x_1} \langle J_y \rangle\, dx \;-\; 2\int_{x}^{\infty} B_x(x',y,h/2)\, dx' \quad . \tag{3-16}$$

In writing Eq. (3-16) we have made use of the antisymmetry in B_x about z=0. Integrating Eq. (3-16) over y and making the change of variables denoted by Eq. (3-2) yields

$$\langle B_z(\xi) \rangle \;=\; \mu \ell_a \int_{\xi}^{1} \langle J_y(\xi') \rangle\, d\xi' \;-\; \frac{2\ell_a}{h\,w} \int_{-w/2}^{w/2} \int_{\xi}^{\infty} B_x(\xi',y,h/2)\, d\xi'\, dy \tag{3-17}$$

for the average B_z field on the arc at ξ.

Since the current in the rails is in the x-direction, it cannot contribute to B_x. Furthermore, we again assume that the rails are infinitely long in the negative x-direction. Then B_x arises only from the current in the arc, and is given by the Biot-Savart law:

$$B_x(\xi,y,h/2) \;=\; \frac{\mu \ell_a}{4\pi} \int_{0}^{1} \int_{-h/2}^{h/2} \int_{-w/2}^{w/2} \frac{\langle J_y(\xi') \rangle\, (h/2-z')\, dy'\, dz'\, d\xi'}{\left[\ell_a^2(\xi-\xi')^2 + (y-y')^2 + (h/2-z')^2\right]^{3/2}} \quad . \tag{3-18}$$

Carrying out the integrations over y' and z' in Eq. (3-18) yields

$$B_x(\xi,y,h/2) \;=\; \frac{\mu \ell_a}{4\pi} \int_{0}^{1} \langle J_y(\xi') \rangle \left[f(w/2+y,0) + f(w/2-y,0) - f(w/2+y,h) - f(w/2-y,h) \right] d\xi' \tag{3-19}$$

where

$$f(y,z) = \ln \left\{ y + \left[\ell_a^2 (\xi-\xi')^2 + y^2 + z^2 \right]^{1/2} \right\} - 1/2 \ln \left[\ell_a^2 (\xi-\xi')^2 + z^2 \right] . \tag{3-20}$$

Further integration of Eq. (3-19) is, of course, not possible without specifying the current distribution in the arc.

Substituting Eq. (3-19) into Eq. (3-17) and performing some rather tedious integrations yields

$$\langle B_z(\xi) \rangle = \mu \ell_a \left\{ \int_\xi^1 \langle J_y(\xi') \rangle \, d\xi' - \frac{1}{2\pi h'} \int_0^1 \langle J_y(\xi') \rangle \, Q \left[(\xi-\xi') \, \ell_a / w \right] d\xi' \right\} \tag{3-21}$$

where

$$h' = h/w \tag{3-22}$$

$$Q(\eta) = \begin{cases} S(\infty) - S(\eta) & , \ \eta \geq 0 \\ S(\infty) - 2S(0) + S(-\eta) , & \eta < 0 \end{cases} \tag{3-23}$$

and the function $S(\eta)$ is

$$\begin{aligned} S(\eta) = {} & \eta \ln \left\{ \frac{(\eta^2 + h'^2)}{\eta^2} \left[\frac{1 + \sqrt{1 + \eta^2}}{1 + \sqrt{1 + h'^2 + \eta^2}} \right]^2 \right\} \\ & + \ln (\eta + \sqrt{1 + \eta^2}) \\ & - (1 - h'^2) \ln (\eta + \sqrt{1 + h'^2 + \eta^2}) \\ & - h'^2 \ln (\eta + \sqrt{h'^2 + \eta^2}) \\ & + 2h' \tan^{-1} (\eta/h') \\ & + 2h' \tan^{-1} \left[\frac{1 + h'^2 + \sqrt{1 + h'^2 + \eta^2}}{h'\eta} \right] \\ & + \eta (\eta - \sqrt{1 + \eta^2} - \sqrt{h'^2 + \eta^2} + \sqrt{1 + h'^2 + \eta^2}) . \end{aligned} \tag{3-24}$$

In the limit that η goes to infinity and zero, $S(\eta)$ takes on the values

$$S(\infty) = \pi h' + 2h' \tan^{-1} (1/h') \qquad (3\text{-}25)$$

$$S(0) = \pi h' - (1 - h'^2) \ln \frac{1 + h'^2}{h'^2} \ln h' \ .$$

Equations (3-7), (3-15), and (3-21) represent the equations for the average pressure in finite-height rail guns. As such, they would replace Eqs. (3-1), (3-3) and (3-4) in the analyses of Refs. 5 and 6. It is a straightforward exercise to show that the two sets of equations become identical in the limit that $h_a = h_r = h$ approaches infinity.

One result of the form of Eqs. (3-15) and (3-21) is that the net force on the arc/projectile system, which is proportional to the integral of $\langle J_y \rangle \langle B_z \rangle$, is independent of the current distribution in the arc. (This characteristic, which had previously been noted for infinitely high rails [10], is derived in the Appendix.) In particular, the net force is the same as if the current was confined to the surface of the arc, which is precisely the assumption used to derive the effective inductance in Section II. Thus, the force can be obtained by calculating L from Eq. (2-14) and substituting the result into Eq. (2-1).

It is interesting to speculate whether the magnetic pressure profile for finite-height rail guns can be adequately approximated by merely scaling the pressure profile obtained for the case of infinitely high rails. The rationale for attempting to do this is the following. In arc models designed for computational efficiency, such as that described in Ref. 6, as well as in models for studying arc instabilities it is often desirable to choose a functional form for the electrical conductivity which simplifies the calculation of the magnetic pressure. It is apparent from the relatively simple form of Eqs. (3-3) and (3-4) that this can be readily achieved for the case of rails with infinite-height. On the other hand, one would be hard pressed to find a conductivity which would lead to a simplification in evaluating $\langle B_z \rangle$ from Eq. (3-21). If the pressure profiles do scale, however, then the analysis for finite-height rails would be a straightforward extension of the analysis of infinite-height rail guns.

From Eq. (2-1) and the definition of j_ρ, we can write the average pressure over the arc due to the electromagnetic forces, which we denote as the magnetic pressure, as

$$\bar{p}_m = \frac{L\, j_o^2\, h_r^2}{2\, h_a w} \quad . \tag{3-26}$$

In the limit that $h_a = h_r = \infty$, $\bar{p}_m$ reduces to

$$\bar{p}_{m\infty} = \frac{\mu\, j_o^2}{2} \tag{3-27}$$

which suggests a scaling factor, f, given by

$$f = \bar{p}_m / \bar{p}_{m\infty} = \frac{L\, h_r^2}{\mu\, h_a w} \tag{3-28}$$

for the same j_o. The question then becomes how well the magnetic pressure gradient

$$d\langle p_m \rangle / d\xi = \ell_a \langle J_y \rangle \langle B_z \rangle \tag{3-29}$$

is approximated by the scaled equation

$$d\, p_{ms}/d\xi = \ell_a\, f\, J_y\, B_z \tag{3-30}$$

where J_y and B_z are solutions of Eqs. (3-3) and (3-4).

To address this question, we consider the case where the conductivity is constant throughout the arc and equal to $\bar{\sigma}$. We also restrict our discussion to equal rail and arc heights since that restriction was imposed in deriving Eq. (3-21). For that case, Equations (3-3) and (3-4) predict that J_y is constant and B_z varies linearly with ξ. If we substitute the solutions into Eq. (3-30) and define a non-dimensional magnetic pressure according to

$$P_m = \frac{p_m\, w}{L\, h_a\, j_o^2} \quad , \tag{3-31}$$

Eq. (3-30) for the scaled pressure becomes

$$d\, P_{ms}/d\xi = 1 - \xi \quad . \tag{3-32}$$

This linear variation is shown as the solid line in Fig. 5. Also shown in the figure are plots of the normalized pressure gradient for two finite-height rail gun geometries corresponding to h' equal to unity and $\ell_a/w = 2$ and 10. These curves were obtained by solving Eq. (3-21) numerically and substituting the result, along with $\langle J_y \rangle$ from Eq. (3-15), directly into Eq. (3-29).

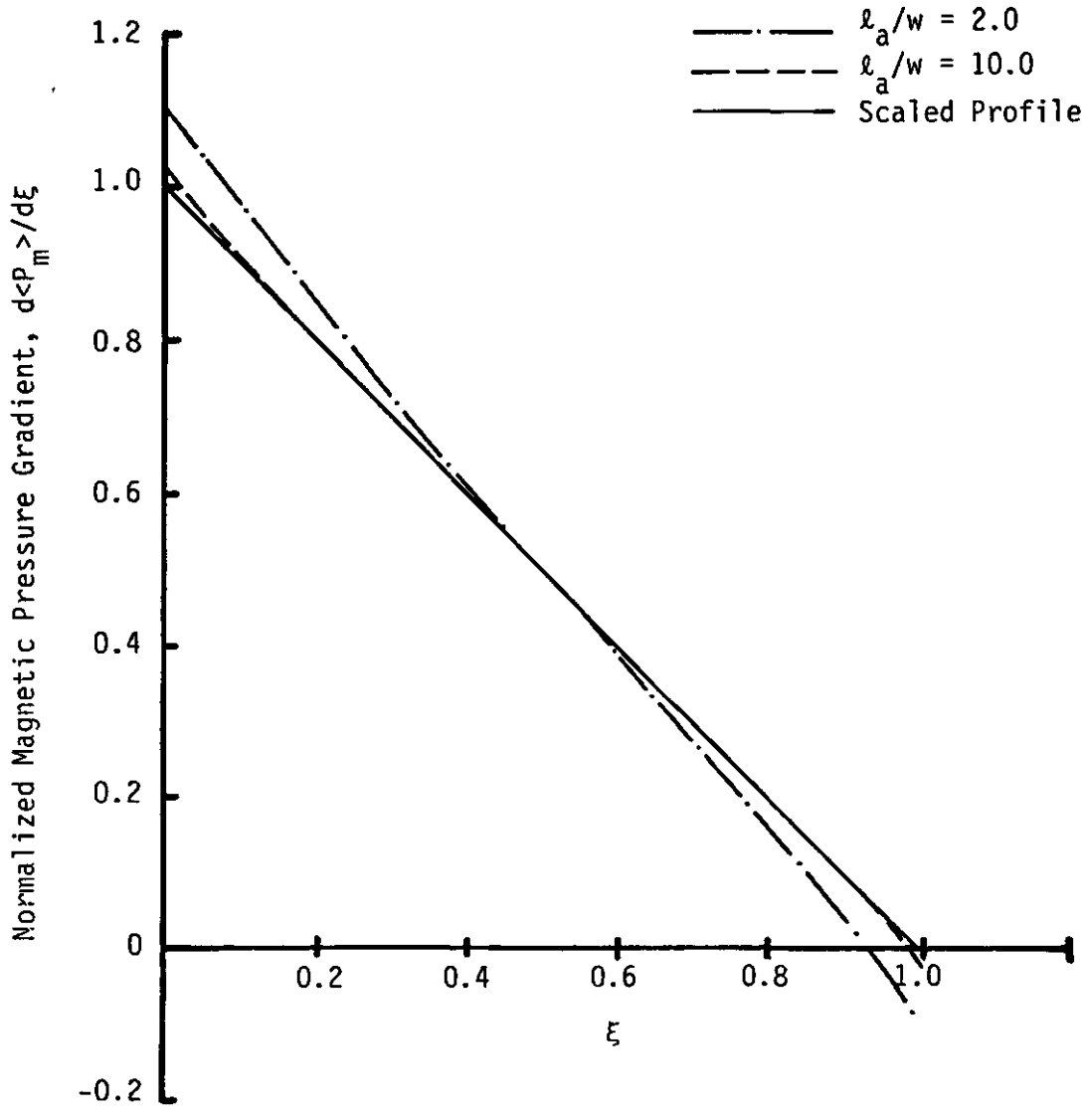

Figure 5. Comparison of Arc Magnetic Pressure Gradients with Scaled Pressure Gradient ($h' = 1.0$, $J_y = -j_o/\ell_a$)

Comparison of the curves in Fig. 5 indicates that the scaled result appears to provide a good representation of the magnetic pressure gradient in finite-height rail guns for typical geometries (h' approximately equal to 1.0, $\ell_a/w \gtrsim 5.0$), at least for the case of uniform conductivity. In general, the agreement is better for larger values of ℓ_a/w. Although it is not shown in the figure, agreement also improves as h' increases, which is to be expected since the scaled curve corresponds to the case where $h' = \infty$.

Figure 6 shows the same set of curves for the case where the current profile in the arc is assumed to vary linearly according to the relation

$$J_y = -2j_o \xi/\ell_a \quad . \tag{3-33}$$

The current variation described in Eq. (3-33) is not chosen to correspond to any realistic physical situation but merely to show how the current profile affects the accuracy of the scaled pressure equation. Again, we note that the scaled pressure gradient profile gives a good approximation to the numerically calculated profile, particularly for large values of ℓ_a/w.

An interesting feature of the exact curves in Figs. 5 and 6 is that the magnetic pressure gradient actually becomes negative near the projectile, corresponding to a reversal in the direction of the B field. This arises because, near the leading edge of the arc, the contribution to the pressure gradient from the current in the rails is exceeded by the contribution from the arc's own current, which tends to 'pinch' the arc in the x-direction.

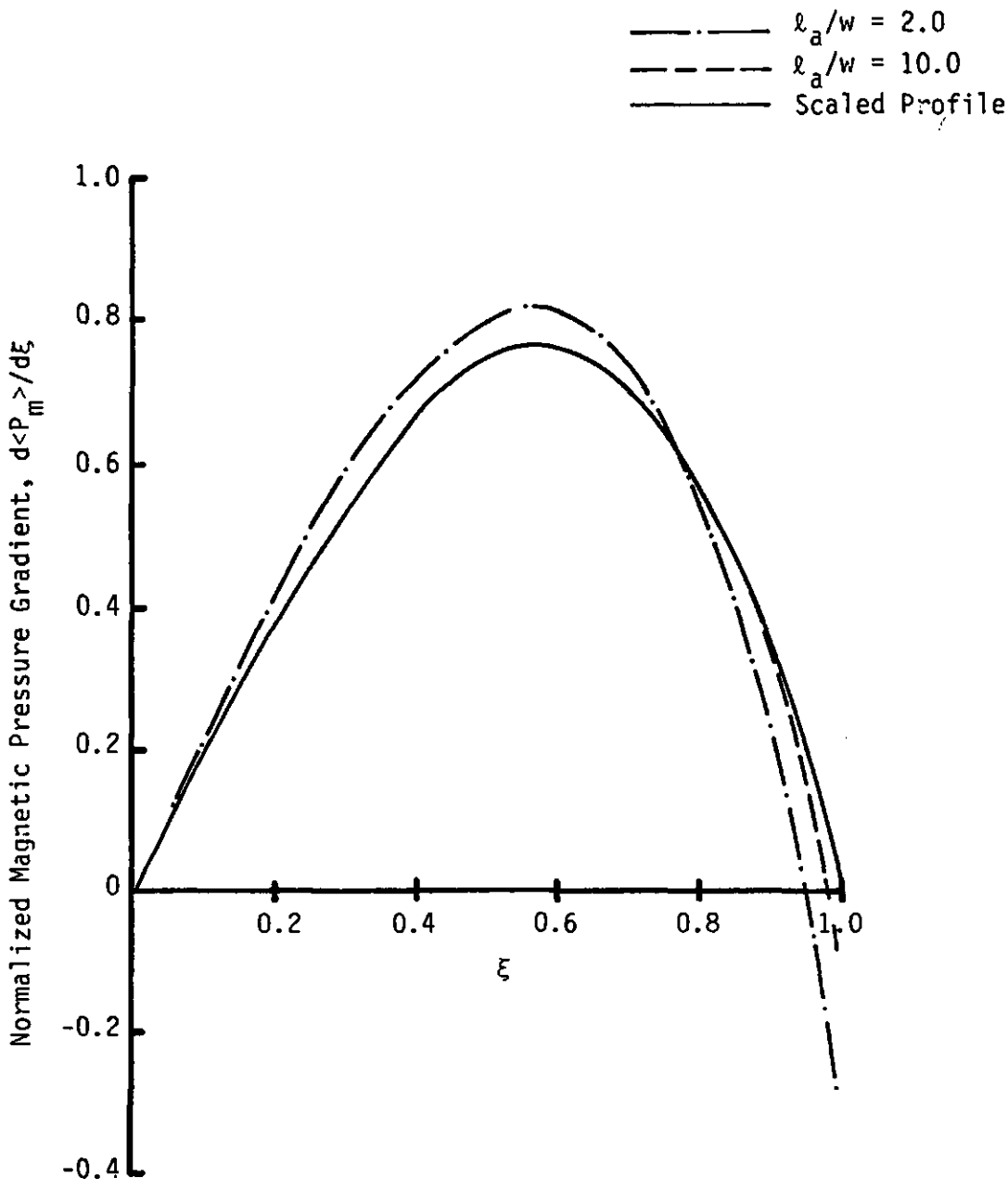

Figure 6. Comparison of Arc Magnetic Pressure Gradients with Scaled Pressure Gradient ($h'=1.0$, $J_y = -2j_o\xi/\ell_a$)

IV. EFFECT OF FINITE-HEIGHT RAILS ON ARC PROPERTIES

In this section, we investigate the extent to which including the effect of the finite height of the rails alters the predictions of the properties of the arc in arc-driven rail guns. To do this we exploit the result of the analysis in Sec. 3, namely, that the magnetic pressure gradient for finite-height rails can be approximated by scaling the pressure gradient for infinite-height rails.

The model we use is the simple model for arc properties derived in Ref. 6. In that model, the momentum equation appropriate for infinite-height rails is used to calculate the pressure profile in an arc with constant electrical conductivity and constant temperature. The temperature, in turn, is taken to be the average temperature in the arc based on the solution in three dimensions of the radiation heat transfer equation with a source term to account for ohmic dissipation in the arc. Several other simplifying assumptions are made and these are discussed in detail in Ref. 6.

Based on the scaling arguments discussed in Sec. III. we can utilize the model of Ref. 6 to study the properties of finite-height rail guns provided that the following substitutions are made

$$\begin{aligned} D &\longrightarrow h_a \\ j_o &\longrightarrow j_o h_r/h_a \\ \mu &\longrightarrow L(h_a/w) \end{aligned} \qquad (4\text{-}1)$$

wherever the parameters D, j_o and μ occur in the model. The first two substitutions are required to obtain the correct ohmic dissipation in an arc where $h_a \neq h_r$. (The theory of Ref. 6 was based on $h_r = h_a = D$.) The substitution for μ assures that the correct scaling of the magnetic pressure, as defined by Eq. (3-28), is achieved.

The specific conditions we analyze are those listed in Table 1 which are based on the RM experiment [3]. The parameter D, equal to $(h_r h_a)^{1/2}$, is used to determine the current per unit height for the infinite-height rail gun calculation. The model requires the specification of either the arc mass or arc length. We have chosen to use the arc length since it is the more readily measured of the two parameters. The estimated value of 10 cm for ℓ_a is consistent with previous studies of the RM experiment.

Table 1. CONDITIONS FOR THE RM EXPERIMENT

SYMBOL	QUANTITY	VALUE
w	Rail Separation	1.27×10^{-2} m
h_a	Arc Height on Rails	1.27×10^{-2} m
h_r	Rail Height	1.91×10^{-2} m
D	Effective Rail Height[+]	1.56×10^{-2} m
m_p	Projectile Mass	3.0×10^{-3} kg
I_o	Current	300 kA
m_o	Mass of Ions and Neutrals	1.1×10^{-25} kg
ℓ_a	Arc Length	0.10 m*

[+] $D = (h_a\ h_r)^{1/2}$, used in the infinite rail height model

* Estimated value

Table 2 shows a comparison of the predictions of the infinite-height model and the finite-height model for various arc properties. The final values for the arc pressure and density denote the values at the projectile surface. As expected, the finite-height rail gun model predicts significantly lower arc pressures and accelerations. Since the two models predict similar temperatures, the density predicted by the finite-height model is also much lower than that for the infinite-height model, resulting in a lower arc mass for a given arc length. On the other hand, the muzzle voltage predicted by the finite-height model is approximately fifty percent higher than that predicted by the infinite-height model. This increase is due to the smaller arc cross-sectional area (by the ratio of h_a/D) used for the finite-height calculation, and to a decrease of about fifteen percent in the arc conductivity.

Since there is a large degree of uncertainty in the experimental value of ℓ_a, Figs. 7 - 10 show graphical comparisons of the predictions of the two models for the arc pressure, temperature, muzzle voltage, and arc mass. These figures clearly demonstrate that including the effect of finite-height rails does not alter the trends predicted by the model: namely, that an increase in arc length (or, equivalently, arc mass) results in decreases in the arc pressure and temperature and in the muzzle voltage of the rail gun.

Table 2. COMPARISON OF MODEL PREDICTIONS FOR RM PARAMETERS

SYMBOL	QUANTITY	VALUE ($h_a/w = \infty$)	VALUE ($h_a/w = 1.0$)
$\bar{p}$	Average Arc Pressure (Nt/m^2)	1.48×10^8	0.94×10^8
p_f	Final Arc Pressure (Nt/m^2)	2.13×10^8	1.39×10^8
a	Arc-projectile Acceleration (m/s^2)	1.40×10^7	0.75×10^7
$\bar{\rho}$	Average Arc Density (kg/m^3)	14.3	9.67
ρ_f	Final Arc Density (kg/m^3)	20.6	14.3
m_a	Arc Mass (kg)	0.29×10^{-3}	0.16×10^{-3}
$\bar{n}_e$	Average Electron Number Density (m^{-3})	1.90×10^{26}	1.27×10^{26}
V_o	Muzzle Voltage (V)	43.	63.
$\bar{T}$	Average Arc Temperature (°K)	33,500	31,800
T_{max}	Maximum Arc Temperature (°K)	53,400	50,700
$\bar{\alpha}$	Average Degree of Ionization	1.46	1.44

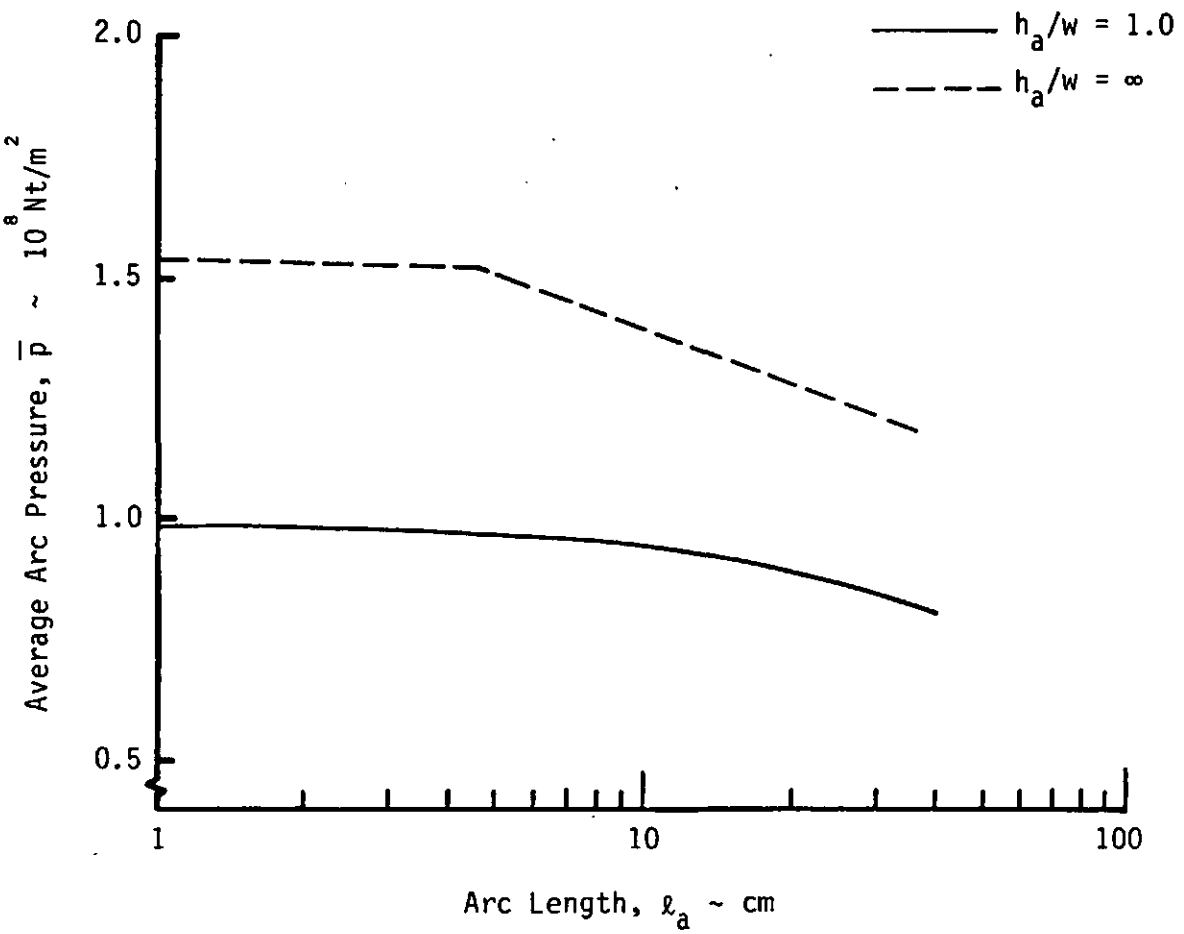

Figure 7. Comparison of Model Predictions for Average Arc Pressure

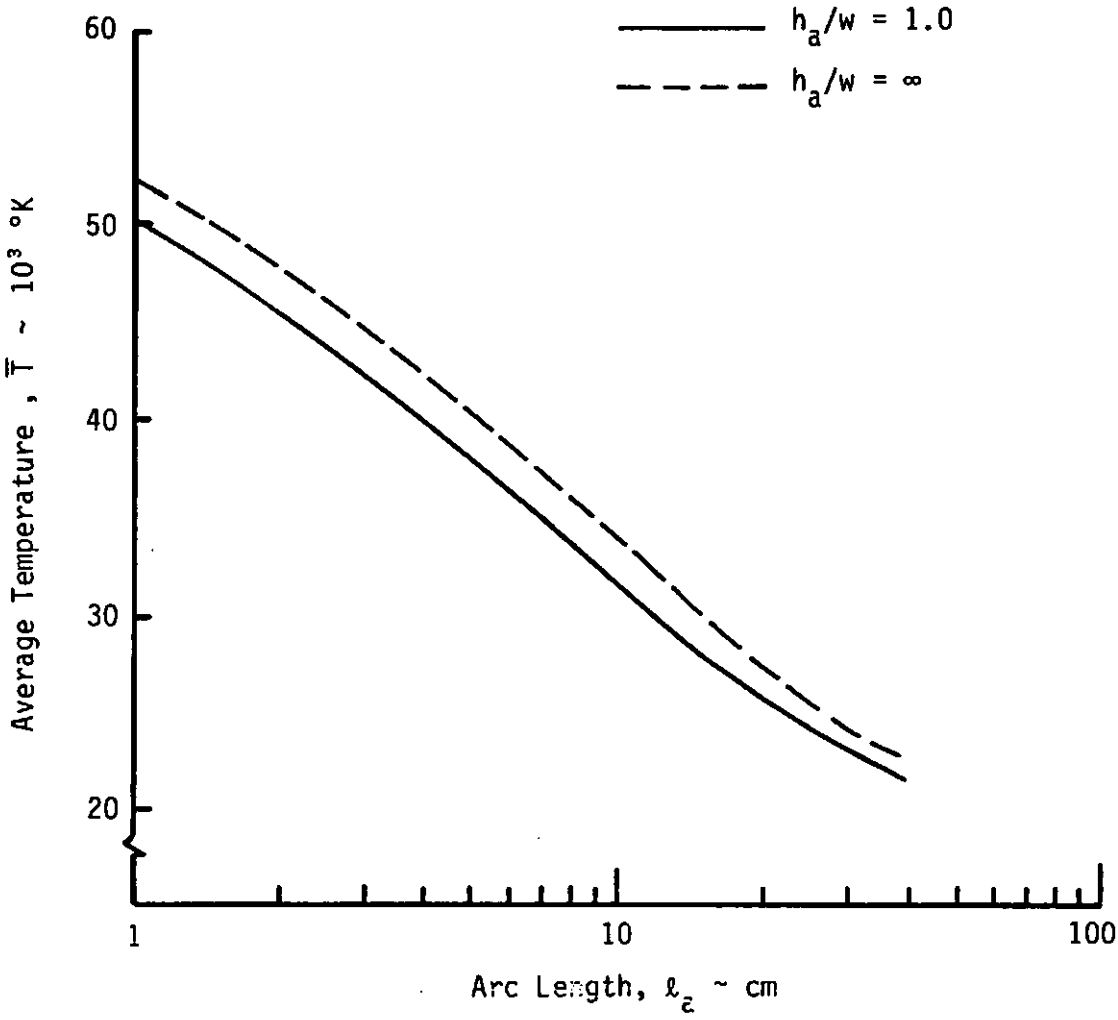

Figure 8. Comparison of Model Predictions for Average Arc Temperature

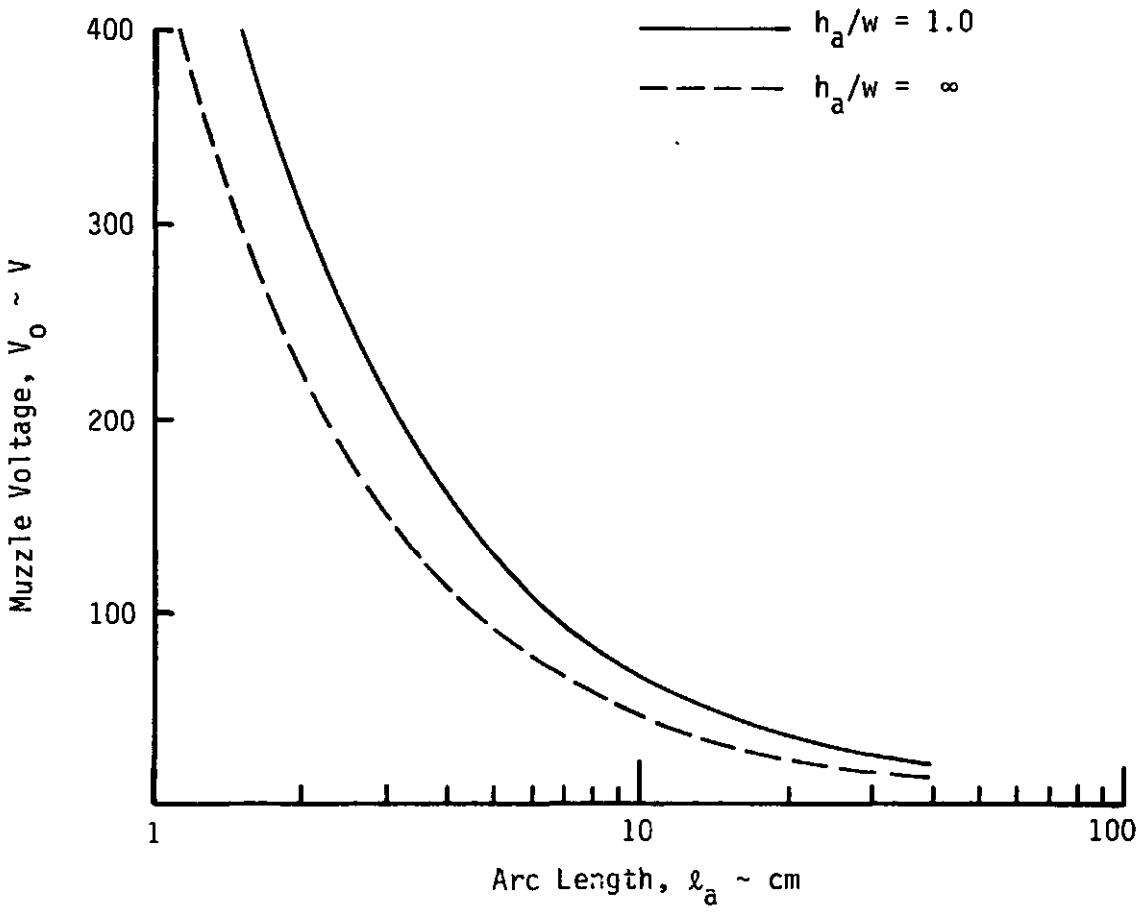

Figure 9. Comparison of Model Predictions for Muzzle Voltage

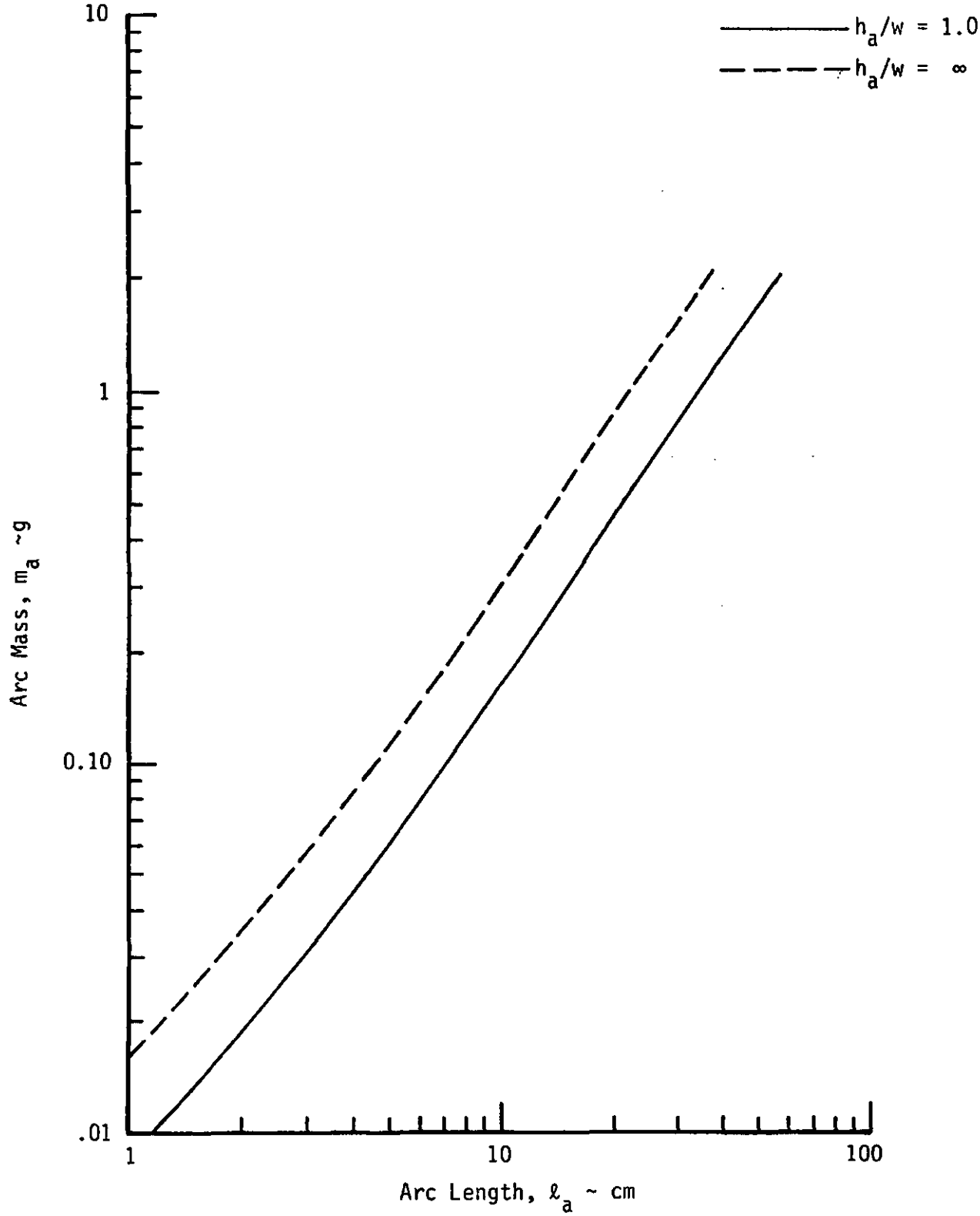

Figure 10. Comparison of Model Predictions for Arc Mass

V. RAIL DAMAGE IN ARC-DRIVEN RAIL GUNS

The successful development of a practical, repetitively fired rail gun requires an understanding of the mechanisms responsible for damage to the rails and the development of techniques to minimize this damage. In this section we discuss some probable causes of rail damage and compare these with the mechanisms responsible for gun-tube erosion in conventional guns. Some recent models developed to analyze erosion in rail guns will also be discussed.

Although a general theory has yet to be formulated, erosion in conventional gun tubes is believed to arise from a combination of the mechanical interaction of the projectile with the gun tube, and the heating of the tube by the hot propellant gases [11,12]. Mechanical erosion, which is relatively independent of the gas temperature, results in a small rate of wear and is most important for low-velocity weapons. For large-caliber, high velocity weapons thermal effects are generally the major causes of barrel erosion. The cyclic heating and cooling of the steel gun tube in a repetitively fired gun leads to a chemical transformation at the surface which makes it particularly susceptible to cracking. If the surface of the gun tube reaches a sufficiently high temperature, then the gun surface will recede as it melts and is wiped away by the flowing projectile gases.

It is likely that thermal and mechanical interactions will also be the major contributors to rail erosion in rail guns. Buckingham has presented a study of mechanical erosion in arc-driven rail guns [13]. His study focuses primarily on the drag and mass loss of the projectile as it interacts with the rails. The calculations are based on gram-sized projectiles which are stressed beyond their yield values and subjected to accelerations on the order of 10^7 m/s^2. For these conditions, he finds that a projectile with a steel sabot will experience significant mass loss due to viscous effects if one attempts to accelerate it to much beyond 4 km/s. Substantially better performance is predicted for a projectile with either a graphite or Teflon sabot, or for a configuration where there is initially a gap between the projectile and rails. An effect which was not considered, and which may be significant, is the leakage of plasma through the gap which could lead to a current-conducting path ahead of the projectile. To seal the gaps and to prevent the projectile from 'bouncing' against the rails, Buckingham suggests the use of ablative bands around the projectile.

---

11. Interior Ballistics of Guns, AMCP 706-150 (US Army Materiel Command, Washington, D.C., 1965) Ch. 3.

12. J. Corner, The Theory of the Interior Ballistics of Guns (Wiley, New York, 1950) Ch. 10.

13. A.C. Buckingham, 'Electromagnetic Propulsion: Drag and Erosion Modeling,' AIAA J. 19, 1422 (1981).

Analogous to the propellant gases in a conventional gun, the plasma arc is the major contributor to rail heating in arc-driven rail guns. There are, however, several important differences. First, the average arc temperature is typically 20,000 to 40,000 °K, whereas the temperature of the propellant gases rarely exceeds a few thousand degrees. Because of the higher temperature, energy is transferred to the rails primarily by radiation. Furthermore, most of the transfer at any point on the rails occurs while the arc is in contact with that point. A secondary source of rail heating is ohmic dissipation in the finite conductivity rails.

Powell has recently completed a study of rail damage arising from these two effects which is based on solutions of the time-dependent diffusion equation [14]. It is assumed in the analysis that once a layer of the rail reaches the melting temperature, it is removed and can no longer absorb radiation. (This is equivalent to the 'melt-and-wipe' hypothesis frequently used to study gun-tube erosion.) The theory provides predictions for the time to initiate melting at the surface and, once the melting temperature has been attained, for the rate of recession of the rail surface as a function of axial position on the rails and the arc properties. The following discussion will help identify the arc properties which are most influential in determining the energy transfer to the rails.

If the rail thickness is large compared to the electrical skin depth, the temperature rise at the surface of the rails during contact with the arc can be approximated by [15]

$$\Delta T = 2q_s \left[t/(\pi \rho_r C_r k_r)\right]^{1/2} + \Delta T_R \qquad (5\text{-}1)$$

where

$$\Delta T_R = \frac{\mu I_o^2}{\pi \rho_r C_r h_a^2} \ln\left(\frac{2 \rho_r C_r}{\mu \sigma_r k_r}\right) \qquad (5\text{-}2)$$

represents the temperature rise due to resistive heating. In Eqs. (5-1) and (5-2), q_s is the value of the radiation flux incident on the surface of the rails, t is the time measured from the arrival of the leading edge of the arc at the point in question, and ρ_r, C_r, k_r and σ_r denote the density, specific heat, thermal conductivity and electrical conductivity, respectively, of the rails. Equation (5-1) is valid until the surface temperature attains the melting temperature. In writing

14. J.D. Powell, 'Thermal Energy Transport from Arc to Rails in an Arc-Driven Rail Gun,' Ballistic Research Laboratory Report No. ARBRL-TR-02530, Oct 83.

15. J.D. Powell, private communication.

this equation, we have noted that magnetic diffusion is generally much faster than thermal diffusion for typical conductors. In addition, we have assumed, conservatively, that the current per unit height of rail in the vicinity of the arc is given by I_o/h_a.

Let's consider an arc in steady state such that the ohmic dissipation in the arc is just balanced by the radiation from its surface. If we assume that the arc has a uniform current density, equal to $I_o/(wh_a)$, and a constant conductivity $\bar{\sigma}$ and that it radiates uniformly from its surface, we can approximate q_s by

$$q_s = \frac{I_o^2 w}{2\bar{\sigma} h_a \ell_a [\ell_a w + \ell_a h_a + w h_a]} \quad . \tag{5-3}$$

The maximum temperature rise at the rail surface occurs just as the trailing edge of the arc passes the point in question, which corresponds to the time

$$t = \frac{[2a\ell_a + v_o^2]^{1/2} - v_o}{a} \tag{5-4}$$

where v_o is the velocity of the leading edge of the arc as it traverses the point, and a is the acceleration of the arc/projectile system

$$a = \frac{L I_o^2}{2(m_a + m_p)} \quad . \tag{5-5}$$

Combining Eqs. (5-1) through (5-5), we can derive an expression for the velocity below which we would expect rail damage due to surface melting. If we take ΔT in Eq. (5-1) to be ΔT_m, the temperature rise required to initiate surface melt, substitute Eq. (5-4) for t and solve for v_o, we get

$$v_o = \frac{1}{2F}\left(\frac{L I_o^2 \ell_a}{m_a + m_p} - F^2\right) \tag{5-6}$$

where

$$F = \frac{\pi \rho_r C_x k_r L}{2(m_a+m_p)} \left[\frac{\bar{\sigma}\, h_a \ell_a (w\ell_a + h_a \ell_a + w h_a)}{w I_o} (\Delta T_m - \Delta T_R) \right]^2 \qquad (5\text{-}7)$$

For copper rails and parameters typical of the RM experiment with an arc length of 10 cm, Eqs. (5-6) and (5-7) yield a v_o on the order of 2 km/s.

Considerable caution should be exercised, however, in applying Eqs. (5-6) and (5-7) to a given experiment since the result is highly dependent on the value assumed for the arc length. For instance, for the RM experiment F^2 is negligible compared to the first term in Eq. (5-6). (This indicates that the increase in velocity during the time required to traverse ℓ_a is much less than v_o.) Then, since $m_p \gg m_a$ and $\bar{\sigma}$ is relatively insensitive to ℓ_a, F varies as ℓ_a^4 for $\ell_a \gg w$ and h_a. Consequently, v_o as predicted by Eq. (5-6) is roughly proportional to $1/\ell_a^2$. Thus, a 20-percent increase in the assumed value of the arc length results in a reduction in v_o of nearly a factor of two. The large sensitivity of the rail temperature rise to the arc length also has been noted by Powell [15]. In addition, we note that v_o is strongly dependent on the current. For a fixed arc conductivity and arc length, it varies as I_o^4.

If we assume that the current is constant and the arc instantaneously achieves its steady-state configuration, then the temperature rise is clearly a maximum near the breech since the transit time there is a maximum. Thus, one would expect the greatest thermal damage to occur near the breech. The velocity v_o can then be interpreted as the velocity with which the projectile must be injected in order to prevent melting of the rails at the breech.

Experimental data does indeed suggest that the damage to the rails in arc-driven rail guns is greatest near the breech. It should be mentioned, however, that the steady-state assumption is probably not valid near the breech [5]. Generation of an arc by the exploding-wire technique leads initially to a highly non-steady situation, with the plasma internal pressure causing the arc to expand against the Lorentz force which acts to force the arc against the projectile. The details of this interaction, which has yet to be examined either experimentally or analytically, will surely influence the energy transport to the rails near the breech.

VI. SUMMARY AND DISCUSSION

In this report, we have developed an equation for the effective inductance per unit length for rail guns with unequal arc and rail heights. The equation provides a simple technique for estimating the net accelerating force, based solely on the current and the gun geometry.

In addition, we have developed a technique for modifying previous models of arc dynamics in rail guns to account for the finite height of the rails. For typical rail gun geometries, the model suggests that the pressure profile for finite-height rails can be well approximated by merely scaling the pressure profile for infinite-height rails, the scaling factor being a function of the effective inductance for the two geometries. Exploiting this result in a simple arc model for the RM experiment, we find that use of the finite-height model leads to considerably lower predictions for the arc pressure, density, acceleration, and arc mass when compared to the predictions for the infinite height model at the same arc length. On the other hand, the use of the finite-height rail gun model leads to a higher prediction for the arc muzzle voltage. The trends indicated by the infinite-height model, however, remain unchanged when the effect of finite-height rails is included.

In future work, the finite-height model developed in this report should be incorporated into the more detailed one-dimensional model described in Ref. 5. This should provide more accurate predictions of the properties of arcs in arc-driven rail guns. Furthermore, the properties predicted by the finite-height model should be used in any future studies of arc stability.

A review of the recent literature has revealed that models have been proposed for analyzing mechanical and thermal damage to the rails in arc-driven rail guns. Although the assumptions used in the models appear reasonable, there is insufficient experimental evidence to determine their validity. The thermal damage model, in particular, is sensitive to parameters, such as the arc length, which are difficult to estimate accurately. Although this limits its utility for reproducing experimental data, the model is valuable nonetheless for indicating the measures that can be taken to reduce thermal energy transfer to the rails. For instance, the model predicts that increasing the arc length (by increasing the arc mass, for example) will lead to considerably lower heat transfer to the rails.

One difficulty with the thermal model is the assumption that the arc is characterized by a steady state. This assumption is probably not justified near the breech where thermal damage to the rails is greatest. Consequently, future studies of rail damage due to the arc should account for the time dependent processes occurring during the generation

of the arc. In addition, the analysis has been conducted only for a single-shot rail gun. A relatively straightforward extension of the model to analyze the cumulative effects of several shots would be particularly useful for determining how rail heating will influence the operation of a repetitively fired gun.

Finally, experimental work needs to be done to characterize the arc and to provide estimates for the extent and type of damage to the rails. Some initial work in this area has been reported [16, 17] and these efforts hopefully will be continued. The work of Jamison et al at BRL is particularly noteworthy. On the basis of tracks left on the conducting rails and light emission from the arc, they conclude that fine structure exists in the current distribution in the arc. The existence of preferred current paths and local 'hot spots' in the arc would significantly affect heat transfer to the rails. Clearly, additional study of this phenomenon, both experimentally and theoretically, would be desirable.

ACKNOWLEDGEMENT

I am grateful to J.D. Powell for several useful discussions and for prepublication access to his work, and to K.A. Jamison and H.S. Burden for the opportunity to discuss their experimental work. The assistance of J.C. Deen, Jr., in programming the numerical computations is gratefully acknowledged.

16. C.A.L. Westerdahl, J. Pinto, G.L. Ferrentino, D.W. Scherbarth, and T. Gora, 'Large-Railgun Residue Material Analyzed by X-Ray Photoelectron Spectroscopy,' IEEE Trans. on Magnetics MAG-19, 53 (1983).

17. K.A. Jamison, H.S. Burden, and M. Marquez-Reines (private communication).

REFERENCES

1. J.P. Barber, 'The Acceleration of Macroparticles and a Hypervelocity Electromagnetic Accelerator,' Ph.D. Thesis (Australian National University, 1972) (Unpublished).

2. R.A. Marshall, 'The Australian National University Rail Gun Project,' Atomic Energy 16, January 1975.

3. S.C. Rashleigh and R.A. Marshall, 'Electromagnetic Acceleration of Macroparticles to High Velocities,' J. Appl. Phys. 49, 2540 (1978).

4. 'Laboratory Demonstration Electromagnetic Launcher - EMACK,' Commissioning Test Results, Westinghouse Research and Development Center, Pittsburgh, PA.

5. J.D. Powell and J.H. Batteh, 'Plasma Dynamics of an Arc-Driven, Electromagnetic Projectile Accelerator,' J. Appl. Phys. 52, 2717 (1981).

6. J.H. Batteh, 'Analysis of a Rail Gun Plasma Accelerator,' Science Applications, Inc., Ballistic Research Laboratory Contract Report No. ARBRL-CR-00478, 1982 (AD A114043).

7. J.D. Powell and J.H. Batteh, 'Two-Dimensional Plasma Model for the Arc-Driven Rail Gun,' J. Appl. Phys. 54, 2242 (1983).

8. J.D. Powell and J.H. Batteh, 'Atmospheric Effects on Projectile Acceleration in the Rail Gun,' J. Appl. Phys. (in press).

9. F.W. Grover, Inductance Calculations (Van Nostrand, New York, 1946) Ch. 10.

10. J.D. Powell and J.H. Batteh, 'Plasma Dynamics of the Arc-Driven Rail Gun,' Ballistic Research Laboratory Report No. ARBRL-TR-02267, 1980 (AD A092345).

11. Interior Ballistics of Guns, AMCP 706-150 (US Army Materiel Command, Washington, D.C., 1965) Ch. 3.

12. J. Corner, The Theory of the Interior Ballistics of Guns (Wiley, New York, 1950) Ch. 10.

13. A.C. Buckingham, 'Electromagnetic Propulsion: Drag and Erosion Modeling,' AIAA J. 19, 1422 (1981).

14. J.D. Powell, 'Thermal Energy Transport from Arc to Rails in an Arc-Driven Rail Gun,' Ballistic Research Laboratory Report No. ARBRL-TR-02530, Oct 83.

15. J.D. Powell, private communication.

16. C.A.L. Westerdahl, J. Pinto, G.L. Ferrentino, D.W. Scherbarth, and T. Gora, 'Large-Railgun Residue Material Analyzed by X-Ray Photoelectron Spectroscopy,' IEEE Trans. on Magnetics MAG-19, 53 (1983).

17. K.A. Jamison, H.S. Burden, and M. Marquez-Reines (private communication).

APPENDIX A

THIS PAGE WAS INTENTIONALLY LEFT BLANK

APPENDIX A

In this Appendix, we show that the net electromagnetic force on the arc/projectile system is independent of the current distribution in the arc for the finite-height-rail model of Sec. III.

The electromagnetic force is

$$F_m = wh\,\ell_a \int_0^1 \langle J_y \rangle \langle B_z \rangle \, d\xi \quad . \tag{A-1}$$

Substituting (3-21) into Eq. (A-1) and using the definitions

$$\begin{aligned} u(\xi) &= \int_0^\xi \langle J_y \rangle \, d\xi \\ u(1) &= -\, j_0/\ell_a \\ u(0) &= 0 \end{aligned} \tag{A-2}$$

yields

$$F_m = \mu wh\,\ell_a{}^2 \left[\frac{u(1)^2}{2} - \frac{R}{2\pi h'} \right] \tag{A-3}$$

where

$$R = \int_0^1 du/d\xi \int_0^1 du/d\xi' \;\; Q[(\xi-\xi')\,\ell_a/w] \, d\xi' \, d\xi \quad . \tag{A-4}$$

If we integrate R by parts with respect to ξ, then repeat the procedure with respect to ξ', and add the results, we obtain

$$R = \frac{1}{2} u(1) \int_0^1 du/d\xi \left\{ Q[(\xi-1)\,\ell_a/w] + Q[(1-\xi)\,\ell_a/w] \right\} d\xi \quad . \tag{A-5}$$

Substituting Eq. (3-23) into Eq. (A-5) and integrating yields

$$R = [S(\infty) - S(0)]\, u(1)^2 \quad . \tag{A-6}$$

Replacing R by this result in Eq. (A-3) and utilizing the definition of u(1) given in Eq. (A-2) yields our final result,

$$F_m = \frac{\mu w h j_o^2}{2} \left[1 - \frac{S(\infty) - S(0)}{\pi h'} \right] . \qquad (A-7)$$

Thus, the net electromagnetic force depends only on the current per unit height of rail and the rail gun geometry.

DISTRIBUTION LIST

No. of Copies	Organization
12	Administrator Defense Technical Info Center ATTN: DTIC-DDA Cameron Station Alexandria, VA 22314
1	Office Under Secretary of Defense Research & Engineering ATTN: Mr. Ray Thorkildsen Room 3D1089, The Pentagon Washington, DC 20301
1	Deputy Under Secretary of Defense Research & Engineering Room 3E114, The Pentagon Washington, DC 20301
3	Director Defense Advanced Research Projects Agency ATTN: Dr. Joseph Mangano Dr. Gordon P. Sigman Dr. Harry Fair 1400 Wilson Boulevard Arlington, VA 22209
1	Office of Assistant Secretary of the Army ATTN: RDA, Dr. Joseph Yang Room 2E672, The Pentagon Washington, DC 20310
1	HQDA (DAMA-ARZ-A/Dr. Richard Lewis) Washington, DC 20310
1	Commander US Army Materiel Development & Readiness Command ATTN: DRCDMD-ST 5001 Eisenhower Avenue Alexandria, VA 22333
1	Commander US Army Materiel Development & Readiness Command ATTN: DRCLDC, Mr. Langworthy 5001 Eisenhower Avenue Alexandria, VA 22333
1	Commander US Army Armament, Munitions & Chemical Command Armament Research & Development Center ATTN: DRSMC-TDC(D) Dover, NJ 07801
6	Commander US Army Armament, Munitions & Chemical Command ATTN: DRSMC-TSS(D) DRSMC-LCA(D), Mr. J.A. Bennett Dr. T. Gora, Dr. P. Kemmy DRSMC-SCA(D), Mr. W.R. Goldstein Dover, NJ 07801
1	Commander US Army Armament, Munitions & Chemical Command ATTN: DRSMC-LEP-L(R) Rock Island, IL 61299
1	Director Benet Weapons Laboratory Armament R&D Center US Army Armament, Munitions & Chemical Command ATTN: DRSMC-LCB-TL(D) Watervliet, NY 12189
1	Commander US Army Aviation Research & Development Command ATTN: DRDAV-E 4300 Goodfellow Boulevard St. Louis, MO 63120
1	Director US Army Air Mobility Research & Development Command Ames Research Center Moffett Field, CA 94035
1	Commander US Army Communications Research & Development Command ATTN: DRSEL-ATDD Fort Monmouth, NJ 07703

DISTRIBUTION LIST

No. of Copies	Organization
1	Commander US Army Electronics R&D Command Technical Support Activity ATTN: DELSD-L Fort Monmouth, NJ 07703
1	Commander US Army Missile Command ATTN: DRSMI-R Redstone Arsenal, AL 35898
1	Commander US Army Missile Command ATTN: DRSMI-YDL Redstone Arsenal, AL 35898
1	Commander US Army Tank Automotive Command ATTN: DRSTA-TSL Warren, MI 48090
1	Director US Army TRADOC Systems Analysis Activity ATTN: ATAA-SL White Sands Missile Range NM 88002
2	Commandant US Army Infantry School ATTN: ATSH-CD-CSO-OR Fort Benning, GA 31905
2	Commander US Army Research Office ATTN: Dr. Fred Schmiedeshoff Dr. M. Ciftan PO Box 12211 Research Triangle Park, NC 27709
1	Commander Naval Air Systems Command ATTN: John A. Reif, AIR 350B Washington, DC 20360
4	Commander Naval Surface Weapons Center ATTN: Mr. H.B. Odom, Code F-12 Dr. M.F. Rose, Code F-04 Mr. P.T. Adams and Mr. D.L. Brunson, Code G-35 Dahlgren, VA 22448
2	Commander US Naval Research Laboratory ATTN: Dick Ford, Code 4774 Dr. I. Vitkovitsky Washington, DC 20375
1	HQ AFSC/SDOA ATTN: XRB (CPT Dennis Kirlin) Andrews AFB, MD 20334
2	AFATL/DLDB (Lanny Burdge, Bill Lucas) Eglin AFB, FL 32542
1	AFATL (Richard Walley) Eglin AFB, FL 32542
1	AFWL (Dr. William L. Baker) Kirtland AFB, NM 87117
1	AFWL/NTYP (John Generosa) Kirtland AFB, NM 87117
1	AFWL/SUL Kirtland AFB, NM 87117
1	AFAPL (Dr. Charles E. Oberly) Wright-Patterson AFB, OH 45433
1	AFAWL/POOS-2 (CPT Jerry Clark) Wright-Patterson AFB, OH 45433
1	Director Brookhaven National Laboratory ATTN: Dr. James R. Powell, Bldg 129 25 Brookhaven Avenue Upton, NY 11973
2	Director Lawrence Livermore National Laboratory ATTN: Dr. R.S. Hawke L-156, Box 808 Livermore, CA 94550

DISTRIBUTION LIST

No. of Copies	Organization
2	Director Los Alamos Scientific Lab ATTN: Dr. Clarence M. Fowler, MS970 Dr. Denis R. Peterson, MS985 Los Alamos, NM 87545
3	NASA-LeRC-MS 501-7 ATTN: Bill Kerslake Frank Terdan Mike Brasher 21000 Brookpark Road Cleveland, OH 44135
1	Boeing Aerospace Company ATTN: J.E. Shrader PO Box 3707 Seattle, WA 94124
1	General Dynamics ATTN: Dr. Jaime Cuadros PO Box 2507 Pamona, CA 91766
3	GT Devices ATTN: Dr. Derik Tidman Dr. Shyke Goldstein Dr. Neils Winsor 5705-A General Washington Drive Alexandria, VA 22312
1	Physics International ATTN: Dr. A.L. Brooks 2700 Merced Street San Leandro, CA 94577
2	R&D Associates ATTN: Mr. Ronald Cunningham Dr. Peter Turchi PO Box 9695 Marina del Rey, CA 90291
1	Science Applications, Inc. ATTN: Dr. Jad H. Batteh 1503 Johnson Ferry RD, Suite 100 Marietta, GA 30062
1	Science Applications, Inc. Corporate Headquarters ATTN: Dr. Frank Chilton 1250 Prospect Plaza La Jolla, CA 92037
1	Unidynamics/Phoenix, Inc. ATTN: W.R. Richardson PO Box 2990 Phoenix, AZ 85062
2	Vought Corporation ATTN: William B. Freeman Charles Haight PO Box 225907 Dallas, TX 75265
2	Westinghouse Research & Development Laboratory ATTN: Dr. Ian R. McNab Dr. Y. Thio Gateway 3 Pittsburgh, PA 15222
2	Massachusetts Institute of Technology Francis Bitter National Magnet Lab ATTN: Dr. Henry H. Kolm, Dr. Peter Mongeau 170 Albany Street Cambridge, MA 02139
1	University of Texas Center of Electromechanics ATTN: Mr. William F. Weldon 167 Taylor Hall Austin, TX 78712

Aberdeen Proving Ground

Dir, USAMSAA
ATTN: DRXSY-D
DRXSY-MP, H. Cohen
Cdr, USATECOM
ATTN: DRSTE-TO-F
Cdr, CRDC, AMCCOM, Bldg E3516
ATTN: DRSMC-CLB-PA
DRSMC-CLN
DRSMC-CLJ-L

THIS PAGE WAS INTENTIONALLY LEFT BLANK

USER EVALUATION OF REPORT

Please take a few minutes to answer the questions below; tear out this sheet, fold as indicated, staple or tape closed, and place in the mail. Your comments will provide us with information for improving future reports.

1. BRL Report Number _____

2. Does this report satisfy a need? (Comment on purpose, related project, or other area of interest for which report will be used.)

_____

_____

_____

3. How, specifically, is the report being used? (Information source, design data or procedure, management procedure, source of ideas, etc.) _____

_____

_____

4. Has the information in this report led to any quantitative savings as far as man-hours/contract dollars saved, operating costs avoided, efficiencies achieved, etc.? If so, please elaborate.

_____

_____

5. General Comments (Indicate what you think should be changed to make this report and future reports of this type more responsive to your needs, more usable, improve readability, etc.) _____

_____

_____

_____

6. If you would like to be contacted by the personnel who prepared this report to raise specific questions or discuss the topic, please fill in the following information.

Name: _____

Telephone Number: _____

Organization Address: _____

_____

_____

FOLD HERE

Director
US Army Ballistic Research Laboratory
ATTN: DRSMC-BLA-S (A)
Aberdeen Proving Ground, MD 21005

NO POSTAGE
NECESSARY
IF MAILED
IN THE
UNITED STATES

OFFICIAL BUSINESS
PENALTY FOR PRIVATE USE, $300

BUSINESS REPLY MAIL
FIRST CLASS PERMIT NO 12062 WASHINGTON, DC
POSTAGE WILL BE PAID BY DEPARTMENT OF THE ARMY

Director
US Army Ballistic Research Laboratory
ATTN: DRSMC-BLA-S (A)
Aberdeen Proving Ground, MD 21005

FOLD HERE